High performance top-emitting OLEDs with copper iodide-doped hole injection layer

Jae-Hyun Lee, Dong-Seok Leem*† *and Jang-Joo Kim*
Dept. of Materials Science and Engineering, and Center for OLED
Seoul Nat'l Univ., Seoul, KOREA
TEL: 82-2-875-2412, e-mail: kuaaa1@snu.ac.kr

Keywords : Top-emitting OLEDs, CuI, Lambertian

Abstract

Efficient top-emitting organic light-emitting diodes were fabricated using copper iodide (CuI) doped NPB as a p-doped hole injection layer to improve hole injection from a silver bottom electrode. The enhanced hole injection is originated from the formation of the charge transfer complex between CuI and NPB. The devices result in high efficiency of 69 cd/A with almost Lambertian emission pattern.

1. Introduction

Top-emitting organic light-emitting diodes (TEOLEDs) are preferred in small size full color active matrix organic light-emitting diodes (AMOLEDs) to increase the aperture ratio of light emission in the displays [1] and [2]. Furthermore, their out-coupling efficiency can be enhanced by using the microcavity effect formed by a highly reflective bottom electrode and a semitransparent top electrode in the devices. A well-designed distributed Bragg reflector with high reflectance in the visible wavelength range or metals such as silver and aluminum have been commonly used as the highly reflective bottom mirror. However, these metal electrodes have low work functions (4.3 eV for Al and 4.6 eV for Ag) which give large injection barrier for holes from the electrodes to hole transporting layers (HTLs).

Various methods have been developed for efficient hole injection. One example is the insertion of a thin insulating layer between the anode and a HTL. The insulator can be either thin metal oxide layers such as evaporated nickel oxides (NiO_x) [3], and silver oxide (AgO_x) [4] formed by UV–ozone treatment of Ag, or organic layers such as CF_x [5]. However these approaches usually require additional equipments and processes that are not used for conventional OLEDs. Another method is the doping of a p-type dopant in HTL. Various p-type dopants such as vanadium oxide (V_2O_5) [6], tungsten oxides (WO_3) [7], molybdenum oxides (MoO_3) [8] and rhenium oxide (ReO_3) [9] were coevaporated with hole transport organic materials to reduce the hole injection barrier. Also halide materials with strong electron affinity such as antimony pentachloride ($SbCl_5$) [10], ferric chloride ($FeCl_3$) [11] or Iodine (I_2) [12] showed enhancement in hole injection.

In this paper, we report a new p-type dopant of copper iodide (CuI) to enhance the hole injection from a Ag metal anode. High efficiency TEOLEDs were realized using the doped HIL. Relatively low melting temperature (606 °C) of CuI than other metal oxides (800 °C for MoO_3 and 1470 °C for WO_3) facilitates coevaporation with organic materials.

2. Experimental

Thermally grown SiO_2 (3000 Å) on Si wafer was used as the substrate and cleaned with acetone and isopropyl alcohol. The TEOLEDs were fabricated by thermal evaporation under 10^{-7} torr without breaking vacuum. A patterned silver (50 nm) electrode was prepared as the bottom contact anode by thermal evaporation through a shadow mask. The organic multilayer structure was formed by sequentially depositing organic layers on the anode, which consists of 10 nm thick CuI doped NPB as the hole injection layer (HIL), 20 nm thick undoped NPB as the hole transport layer (HTL), 25 nm thick *N*,*N*′-dicarbazolyl-4,4′-biphenyl (CBP) doped with 6 wt% tris-(2-

* Corresponding author. e-mail : jjkim@snu.ac.kr
† Current address : Dept. of Chemistry, Imperial College-London South Kensington Campus, London, U. K.

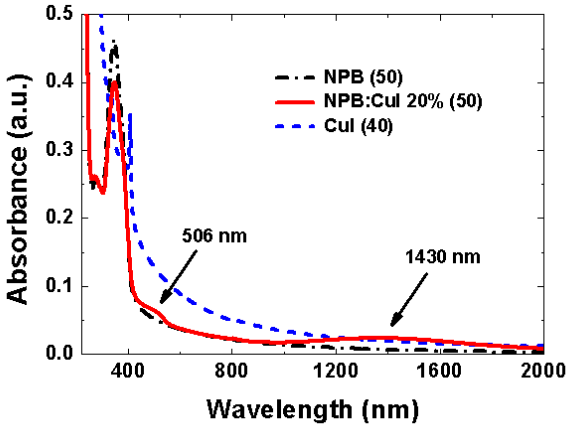

Fig. 1. UV–Vis–NIR absorption spectra of CuI (dashed line), undoped NPB (dot-dashed line) and CuI 20 wt% doped NPB films (solid line), respectively.

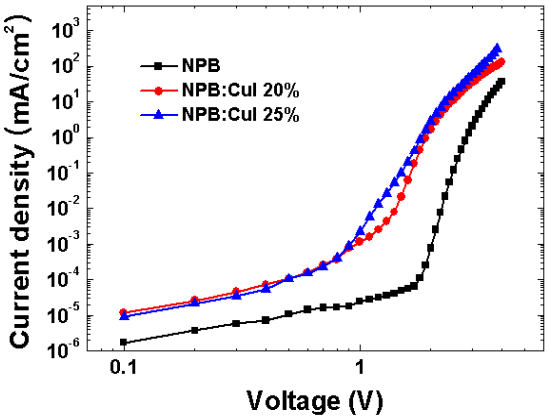

Fig. 2. Current density–voltage characteristics of the hole only devices [Ag (50 nm)/NPB:CuI X% (80 nm)/NPB (20 nm)/Ag (50 nm)] with the doping concentration of 0 wt% (rectangle), 20 wt% (circle) and 25 wt% (triangle), respectively.

phenylpyridyl)iridium(III) ($Ir(ppy)_3$) as the emitting layer (EML), 7 nm thick 2,9-dimethyl-4,7-diphenyl-1,10-phenanthroline (BCP) as the hole blocking layer (HBL), and 44 nm thick tris-(8-hydroxyquinoline)aluminum (Alq_3) as the electron transport layer (ETL), respectively. Ytterbium (1 nm) and silver (20 nm) were used as the cathode to achieve efficient electron injection and semi optical transmittance. Finally 45-nm-thick Alq_3 was deposited as the capping layer to enhance the out-coupling efficiency of the device. The fabricated devices were encapsulated prior to the measurement.

The current density–voltage–luminance (*J–V–L*) characteristics of the devices were measured by a Keithley 2400 semiconductor parameter analyzer and a Photo Research PR-650 spectrophotometer. The absorption spectra were measured by UV–Vis–NIR spectrophotometer Cary 5000. Angular distribution of intensity and spectra were measured by an optical fiber and a S2000 miniature fiber optic spectrometer (Ocean Optics).

3. Results and discussion

Fig. 1 shows the UV–Vis–NIR absorption spectra of the CuI, undoped NPB and 20 wt% CuI doped NPB films. The absorption spectrum of the undoped NPB film shows only absorption peak by π–π* transition near 400 nm wavelength. In contrast, the absorption spectrum of the CuI doped NPB film shows additional absorption peaks at around 506 nm and 1430 nm, which indicates the formation of charge transfer (CT) complexes [7] and [9]. Enhanced hole injection from the Ag anode to HTL through CuI doped NPB HIL was confirmed using hole only devices with the device structure of Ag/NPB:X% CuI (80 nm)/NPB (20 nm)/Ag (50 nm). Fig. 2 shows *J–V* characteristics of the hole only devices consisting of 0, 20 and 25 wt% CuI doped HILs, respectively. The devices with a CuI doped HIL exhibit significantly enhanced the hole injection compared to the device without the CuI doped layer. The turn-on voltage for hole injection was reduced by about 1 V and current density is dramatically enhanced at low voltage region.

To understand the formation of CT complexes of

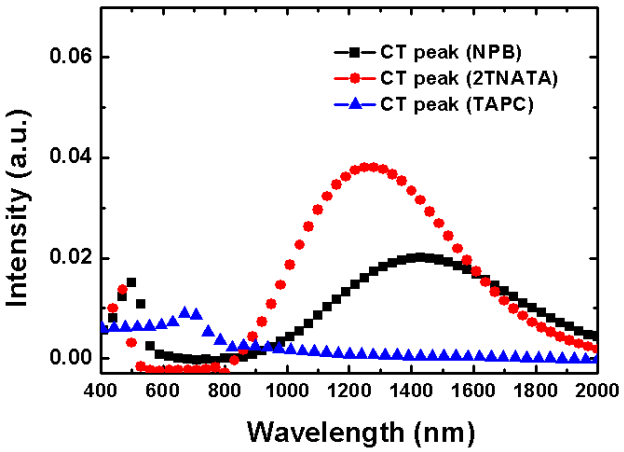

Fig. 3. The difference of absorbance between 20 wt% CuI doped HIL (50 nm) and undoped HIL (50 nm) for NPB (rectangle), 2TNATA (circle) and TAPC (triangle) as the hole transporting materials, respectively.

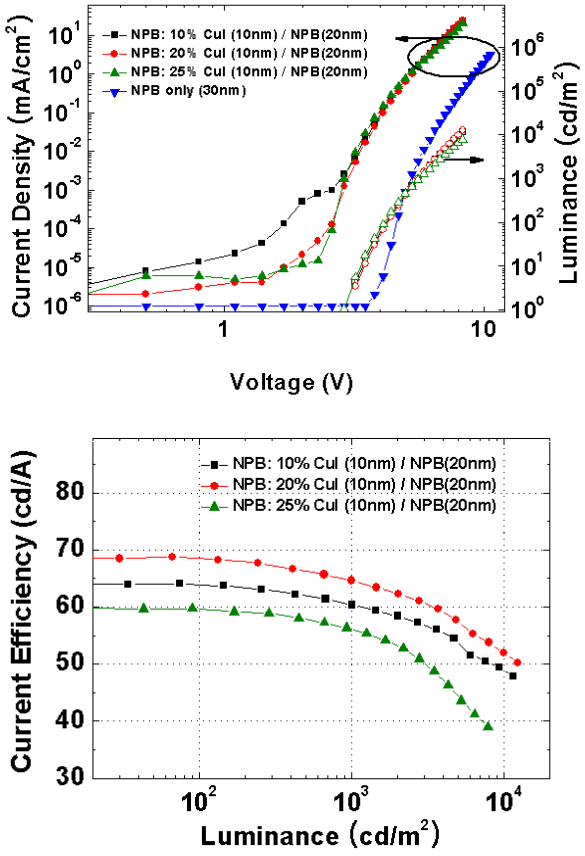

Fig. 4. (a) Current density–voltage–luminance characteristics and (b) current efficiency–luminance of the TEOLEDs adopting CuI doped NPB HILs with the doping concentration of 0 wt% (inverse triangle), 10 wt% (rectangle), 20 wt% (circle) and 25 wt% (triangle).

CuI with hole transporting materials, we doped CuI in the three different hole transport materials of NPB, 4,4′,4″-tris-(*N*-(2-naphthyl)-*N*-phenyl-amino)triphenylamine (2-TNATA) and 1,1-bis-(4-methylphenyl)-aminophenyl-cyclohexane (TAPC).

Fig. 3 shows the difference absorption spectra between CuI doped (20 wt%) HIL and undoped HIL. Apparently 2-TNATA and NPB films doped with CuI form charge transfer complexes effectively. However, TAPC shows little change in absorption by the doping. This behavior can be easily understood based on the energy levels of the materials. NPB and 2-TNATA have high HOMO level of 5.4 eV and 5.0 eV, respectively. On the other hand TAPC has much lower HOMO level of 5.8 eV [13]. These results indicate that the Fermi level of p-type CuI is located between the HOMO levels of NPB and TAPC, which is consistent with the recent report of the Fermi level of CuI [14].

Fig. 4a shows current density–voltage–luminance characteristics of the TEOLEDs consisting of Ag/NPB:X% CuI (10 nm)/NPB (20 nm)/CBP:6 wt% $Ir(ppy)_3$ (25 nm)/BCP (7 nm)/Alq_3 (44 nm)/Yb (1 nm)/Ag (20 nm). The undoped 20 nm thick NPB layer was inserted between HIL and EML to prevent the quenching of exciton at the interface between the doped NPB and EML. The device without CuI doped HIL requires high voltage to inject current through the device and no light was detected up to 10 V, indicating that the hole injection is very small if the doped injection layer is absent. However much improved luminance in the devices with CuI doped HIL indicates that hole injection becomes efficient by the doping. Turn-on (at 1 cd/m^2) and operating voltage (at 1000 cd/m^2) were 2.9 V and 5.6 V, respectively. The current efficiency as a function of luminance is shown in Fig. 4b. All the devices with CuI doped NPB layer showed high current efficiencies. The maximum current efficiency of 69 cd/A was achieved from the device with the 20 wt% CuI doped HIL at 0.14 mA/cm^2. The efficiency corresponds to the external quantum efficiency of 17.5% as the angular dependence of emission intensity from the device is Lambertian. The current efficiency was enhanced by about 10% if the glass cap is removed. Roll-off of the efficiency was not significant in the device with the efficiency of 64.6 cd/A at 1000 cd/m^2, and 57.5 cd/A even at 5000 cd/m^2. The highest luminance efficiency was obtained by setting the normal direction resonant wavelength at about 20 nm longer than the peak wavelength of the intrinsic emission as described by Wu et al. [2]. The devices with different doping concentrations in NPB resulted in lower current efficiency, which can be interpreted based on optical effect related to the shift of recombination zone and less charge balance in the devices coming from the variation of hole injection current. The EL emission spectra and *J–V* characteristics do not change much with doping concentration. However, increasing doping concentration can lead to the shift of the recombination zone toward the hole blocking layer because the hole transport becomes faster with increasing doping concentration as shown in Fig. 2. Our optical calculation showed that the external quantum efficiency increases significantly as the recombination zone shifts toward the HBL without changing the emission spectrum. Therefore, the external quantum efficiency is improved with increasing doping concentration. If the hole transport is too fast, however, the recombination zone can

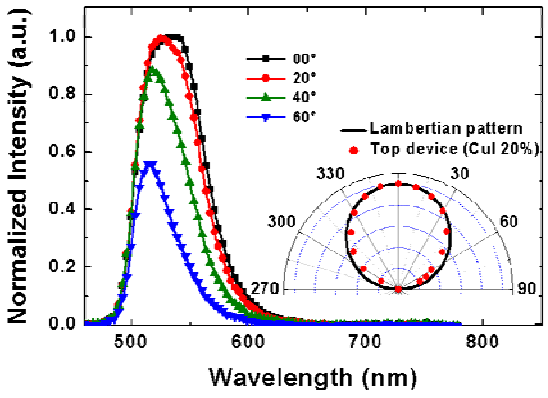

Fig. 5. Spectra of TEOLEDs at different viewing angles. Inset: angular distribution of EL intensity for the TEOLEDs.

penetrate into the HBL to reduce the efficiency again, which is the case for 25% doping. These are the reasons why the 20% doping gives the highest efficiency.

Angular dependence of emission spectrum and intensity of TEOLEDs is important because they are sensitive to the dimension of the devices and related to the viewing angle problem. Fig. 5 shows the electroluminescence spectra measured at the current density of 20 mA/cm^2 at different viewing angles of 0°, 20°, 40° and 60° off from the normal direction for the device with CuI 20 wt% doped HIL. The peak wavelength shifts from 537 nm at 0° to 516 nm at 60°. This spectrum shift with viewing angle might be originated from the microcavity effect of TEOLEDs [15]. It is interesting to note that the angular distribution of the EL intensity of the CuI doped TEOLEDs is similar with the Lambertian distribution as shown in the inset of Fig. 5, while usual TEOLEDs have a distribution with enhanced intensity in the forward direction. The spectrum shift and angular distribution of the emission could be improved by an optimization of the reflectance of the cathode and the thickness of each organic layer.

4. Summary

We have developed a new p-type dopant of CuI and demonstrated high efficiency top-emitting OLEDs using CuI doped NPB as the HIL. Hole injection from the Ag metal anode to NPB was dramatically enhanced by the formation of charge transfer complex between NPB and CuI. The device with 20 wt% CuI doped HIL showed high current efficiency of 69 cd/A, EQE of 17.5% at 0.14 mA/cm^2 and operating voltage of 5.6 V at 1000 cd/m^2. The angular distribution of EL intensity is close to the Lambertian.

This paper was presented in Organic Electronics. (doi:10.1016/j.orgel.2008.05.011)

5. References

[1] V. Bulović, G. Gu, P.E. Burrows, S.R. Forrest and M.E. Thompson, *Nature* **380** (29) (1996).
[2] C.-J. Yang, S.-H. Liu, H.-H. Hsieh, C.-C. Liu, T.-Y. Cho and C.-C. Wu, *Appl. Phys. Lett.* **91** (253508) (2007).
[3] H. Kanno, Y. Sun and S.R. Forrest, *Appl. Phys. Lett.* **86** (263502) (2005).
[4] C.-W. Chen, P.-Y. Hsieh, H.-H. Chiang, C.-L. Lin, H.-M. Wu and C.-C. Wu, *Appl. Phys. Lett.* **83** (5127) (2003).
[5] H. Peng, J. Sun, X. Zhu, X. Yu, M. Wong and H.-S. Kwok, *Appl. Phys. Lett.* **88** (073517) (2006).
[6] X.L. Zhu, J.X. Sun, H.J. Peng, Z.G. Meng, M. Wong and H.S. Kwok, *Appl. Phys. Lett.* **87** (153508) (2005).
[7] C.-C. Chang, M.-T. Hsieh, J.-F. Chen, S.-W. Hwang and C.H. Chen, *Appl. Phys. Lett.* **89** (253504) (2006).
[8] J. Cao, X.Y. Jiang and Z.L. Zhang, *Appl. Phys. Lett.* **89** (252108) (2006).
[9] D.-S. Leem, H.-D. Park, J.-W. Kang, J.-H. Lee, J.-W. Kim and J.-J. Kim, *Appl. Phys. Lett.* **91** (011113) (2007).
[10] C. Ganzorig and M. Fujihira, *Appl. Phys. Lett.* **77** (4211) (2000).
[11] J. Endo, T. Matsumoto and J. Kido, *Jpn. J. Appl. Phys. Part 2* **41** (L358) (2002).
[12] F. Huang, A.G. MacDiamid and B.R. Hsieh, *Appl. Phys. Lett.* **71** (2415) (1997).
[13] M. Aonuma, T. Oyamada, H. Sasabe, T. Miki and C. Adachi, *Appl. Phys. Lett.* **90** (183503) (2007).
[14] A.R. Kumarasinghe, W.R. Flavell, A.G. Thomas, A.K. Mallick, D. Tsoutsou, C. Chatwin, S. Rayner, P. Kirkham, S. Warren, S. Patel, P. Christian, P. O'Brien, M. Grätzel and R. Hengerer, *J. Chem. Phys.* **127** (114703) (2007).
[15] N. Tessler, S. Burns, H. Becker and R.H. Friend, *Appl. Phys. Lett.* **70** (556) (1997).